2019 American Control Conference (ACC)
Philadelphia, PA, USA, July 10-12, 2019

Beyond Quantization in Iterative Learning Control: Exploiting Time-Varying Time-Stamps

Nard Strijbosch, Tom Oomen

Abstract— **Equidistant sampling in control system may lead to quantization errors for certain measurement equipment, e.g., encoders. The aim of this paper is to develop an Iterative Learning Control (ILC) framework that eliminates quantization by exploiting time stamping. The developed ILC framework employs the non-equidistant time stamps in a linear time-varying (LTV) approach. Since the data at the time-stamps does not suffer from quantization, unparalleled performance can be achieved, while the intersample behaviour is bounded by definition. A simulation example confirms superiority of the ILC framework which employs time stamping.**

I. Introduction

Iterative learning control (ILC) can achieve high performance for systems that perform repetitive tasks [1], [2]. The key idea of ILC is to iteratively determine an input signal that compensates for the reproducible part of the error, by learning from the error signal observed during previous iterations of the same task.

In feedback controller design the system is often assumed to be LTI, which is justified by the low performance. When applying a feedback controller, the magnitude of the error will remain substantial compared to the quantization level. This justifies that the quantization effect and corresponding nonlinear system dynamics are neglected. Consequently, this allows to exploit LTI controller design techniques such as loop-shaping control design approaches through, for example, Nyquist diagrams, and Bode-diagrams [3].

Due to the significant performance improvement that ILC achieves, the LTI assumption may no longer be justified, since quantization effects have a substantial contribution to the converged error signal. Indeed, when applying ILC on a mechatronic system the magnitude of the error can be reduced to the quantization level, see [4]. Hence, in [4] nonlinear quantization effects can no longer be neglected. However, the quantization error generally is not taken into account in the analysis or design of ILC. Besides a formal nonlinear analysis, the error caused by quantization can be considered as an extra noise term, e.g. as in [5] dither can be considered to randomize the quantization error. Since trail-varying noise terms are amplified by ILC [6], [7], quantization is expected to deteriorate the performance.

Measurement data from an encoder that stores the time instance, i.e., time stamp, of each change in counter value does not suffer from quantization [8]. The discrete data points are non-equidistant in time and, therefore, cannot not be implemented in an LTI control setting.

Although ILC has been substantially developed, at present quantization effects have not been analysed, consequently also not been addressed in ILC. The aim of this paper is to analyse the effect of quantization in ILC, and a new ILC framework is developed that eliminates these effects. Moreover, the opportunity of offline computations in ILC is exploited such that exact time-stamped measurement data from incremental encoders can be used.

The main contribution of this paper is a new framework for ILC that exploits time stamps to eliminate quantization effects. The potential of time-stamped ILC is enlightened by means of the following contributions.

- C1 In Section II, the time-stamped ILC problem is introduced. Besides its novelty to eliminate quantization errors, it by definition bounds the intersample behaviour, see [9] for intersample behaviour in ILC and [10] for intersample behaviour in feedback control.
- C2 In Section III, a theoretical framework for the analysis of time-stamped ILC setups is provided.
- C3 In Section IV, a design procedure for time-stamped ILC is outlined which ensures monotonic convergence in the 2-norm, thereby inline with common ILC approaches.
- C4 In Section V, a simulation example reveals that the developed ILC framework that exploits time-stamps is superior to commonly used ILC implementations.

All proofs are ommitted due to space limitations and will be published elsewhere.

A. Notations and Definitions

The p-norm of a vector x is given by $\|x\|_p := (\sum_{i=1}^{n} |x_i|^p)^{\frac{1}{p}}$ where $x \in \mathbb{R}^n$ is given by $x := \begin{bmatrix} x_1, x_2, ..., x_n \end{bmatrix}^T$. The sets $\mathbb{N}$, and $\mathbb{Z}$ denote the set of positive integers, and the set of all integers, respectively. To a infinite sequence of spaces X, i.e., $\{Y_k\}_{k\in\mathbb{N}}$ with $Y_k \in X$ the space ℓ_p can be associated consisting of the infinite sequences $y = (y_0, y_1, y_2, ...)$, with $y_k \in X, k \in \mathbb{N}$, with finite ℓ_p-norm, i.e., $\|y\|_{\ell_p} = \left(\sum_{i=0}^{\infty} \|y_i\|_p^p\right)^{\frac{1}{p}} < \infty$.

Throughout, $t \subset \mathbb{Z}$ and $t_c \subset \mathbb{R}$ denotes discrete time and continuous time respectively. In block diagrams, continuous time signals are represented by solid lines, slow sampled discrete time signals are represented by dashed lines and fast sampled discrete-time signals are represented by dotted lines. All systems are assumed to be single-input single-output, finite dimensional and linear time invariant (LTI).

Definition I.1 (Monotonic convergence towards a fixed point) A sequence $\{Y_i\}_{i\in\mathbb{Z}_{\geq 0}}$, $Y_i \in X$ is said to converge

Nard Strijbosch and Tom Oomen are with the Control Systems Technology Group, Departement of Mechanical Engineering, Eindhoven University of Technology, P.O. Box 513, 5600 MB Eindhoven, The Netherlands, e-mail: n.w.a.strijbosch@.tue.nl, t.a.e.oomen@tue.nl. This work is part of the research programme VIDI with project number 15698, which is (partly) financed by the Netherlands Organisation for Scientific Research (NWO).

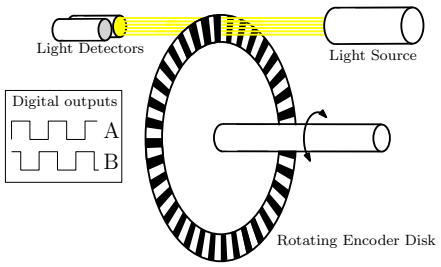

Fig. 1: Schematic representation of incremental encoder

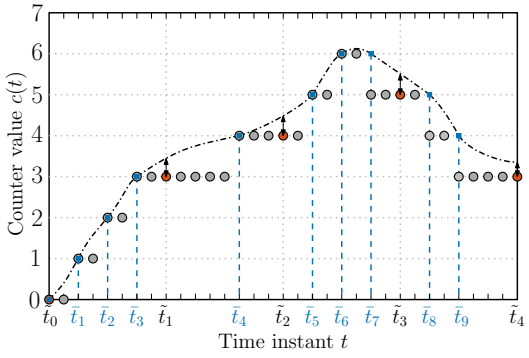

Fig. 2: Counter value of encoder corresponding to the position indicated by (-··-) The encoder operates at a very high equidistant sampling rate, indicated by the circles. The feedback control system operates at a lower equidistant sampling rate (●). Line-transitions are indicated by blue squares (■) and corresponding time-stamps $\bar{t}_i$. These are exact, i.e., not subject to quantization error. In contrast, data points used by the feedback control system, clearly suffer from quantization, indicated by (◂▸).

monotonically, in a given p-norm, to a unique fixed point $Y_\infty \in X$ if there exists a $\kappa \in [0, 1)$ such that

$$\|Y_{j+1} - Y_\infty\|_p \leq \kappa \|Y_j - Y_\infty\|_p \tag{1}$$

is satisfied for all $j \in \mathbb{Z}_{\geq 0}$.

Definition I.2 (Closed p-norm ball) Given a space X and corresponding p-norm, the closed p-norm ball with centre $c \in X$ and radius $d \in \mathbb{R}_{\geq 0}$ is defined by

$$\mathcal{B}_p(c, r) := \{x \in X | \|x - c\|_p \leq d\} \tag{2}$$

II. Problem Formulation

A. Optical incremental encoders

Incremental position encoders are often used to measure the position in mechatronic systems [11], since they can easily be implemented. In Fig. 1, a schematic overview is presented of an incremental encoder. The main components are a slotted disk or strip in linear optical incremental encoders, a light source and two light detectors. The slots in the disk are all equidistant. The light source is aimed at the light detectors. Depending on the position of the encoder disk the slots either obstruct the light or allow the light through. The output of the light detectors are two signals (A,B) which indicate if the light is perceived or not by the light detector. Typically, the two signals have a phase-difference of 90° with respect to each other when velocity is constant. This allows the encoder to detect the direction of the rotation. At

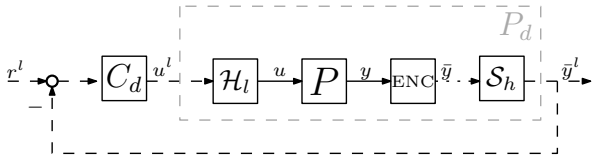

Fig. 3: Block scheme of feedback control scheme with incremental encoder.

a very high sampling rate, f_h, ($\mathcal{O}(f_h) = 10^6 - 10^8$ Hz) the digital signals (A, B) are evaluated and it is determined if one of the signal changed, i.e. if a line-transition occurred in-between two time-instants. A counter keeps track of the number of line transitions taking the direction into account, i.e., when rotating in the positive direction the counter value increases, when rotating in the negative direction the counter value decreases.

A sequence of points detected by the encoder is exemplified in Fig. 2. The value of the counter $c(t)$ can be converted to a position $\bar{y}(t)$, using $\bar{y}(t) = \Delta_e c(t) + y_0$, where y_0 is the initial position of $y(t)$ and $\Delta_e \in \mathbb{R}_{>0}$ related to the width of the encoder slots. Without loss of generality y_0 is assumed to be zero. Due to the width of the encoder slots the difference between the actual position $y(t)$ and $\bar{y}(t)$ is bounded such that $|y(t) - \bar{y}(t)| < \Delta_e$. However, at the time-instant of the line transition the measurement is exact, these time-instances are referred to as time-stamps. In practice, a line transition is detected if $|c(t_i - 1) - c(t_i)| = 1$ with corresponding time-stamp t_i. In Fig. 2 these points are indicated by blue squares (■). The time-stamps corresponding to the line transitions are denoted by $\bar{t} \subset t$. Due to the high sampling rate f_h of the encoder the error at the time-stamps is relatively small, i.e., $|y(\bar{t}_i) - \bar{y}(\bar{t}_i)| << \Delta_e$.

B. Incremental encoders in control setup

Incremental encoders are generally implemented in a feedback system as depicted in Fig. 3, where P represents a continuous-time plant with input $u \in \mathbb{R}$ and position output $y \in \mathbb{R}$. The encoder is represented by the ENC block with output $\bar{y}$. The discrete-time feedback controller C_d is implemented at a sampling frequency f_l, ($\mathcal{O}(f_l) = 10^3 - 10^4$ Hz), with sampling instances defined by $\tilde{t} \in t$. The real-time computations performed by the controller limit this sampling frequency. The ideal sampler $\mathcal{S}_l^*$ connects the discrete-time output of the encoder to the discrete-time controller, and is defined by

$$\mathcal{S}_l^* : \bar{y}(t_i) \mapsto \bar{y}^l(\tilde{t}_i), \quad \bar{y}^l(\tilde{t}_i) = \bar{y}(m\tilde{t}_i), \tag{3}$$

where $t_i, \tilde{t}_i \in t$, and $m \in \mathbb{N}$ denotes the ratio between the sampling frequency of the encoder and the sampling frequency of the feedback control system, i.e., $f_h = M f_l$. The zero-order-hold $\mathcal{H}_l$ connects the digital output of the controller to the analogous input of the plant, given by

$$\mathcal{H}_h : u^l(\tilde{t}) \mapsto u(t_c), u(t_i l + \tau) = u^l(t_i), \tau \in [0, h_l) \tag{4}$$

here $h_l = \frac{1}{f_l}$ denotes the sampling time of the feedback controller.

The quantization effect is non-linear which in common analyse and design procedures of this type of feedback control systems is neglected, i.e., $\bar{y}(t_c) = y(t_c), t_c \in \mathbb{R}_{\geq 0}$. This assumption makes the system linear. However, this can

only be justified if the accuracy of the encoder is sufficiently small compared to the measured error. This assumption allows to determine a discrete-time LTI plant P_d from P, which is used in the analyse or design procedures. This leads to reasonable results, as neglecting the quantization does not lead to instability, although performance will be affected [12], [13].

By using the exact measurement data at the time-stamps $\bar{t}_i, i \in \mathbb{N}$ the quantization effects would be mitigated. However, this data is non-equidistant in time, which makes the system linear time varying (LTV). In [14], a preliminary study is considered to exploit the measurement data at the time stamps to improve equidistant sample instances in real-time using a polynomial approximation through the exact measurement data at the time-stamps. This reduces quantization, especially for real-time purposes. For ILC, a different approach is considered in the next section.

C. What about incremental encoders in ILC?

C.1. LTI ILC

ILC is a batch-to-batch control strategy that is implemented on systems that perform repetitive tasks. The key idea is that the error during each task is highly reproducible, and can therefore be compensate by learning from previous tasks, also referred to as trials. The cause of the reproducible part in the error is a trial invariant disturbance r, which for motion systems could for instance be the reference signal during the task. ILC allows for offline computations in between tasks to determine a control input that aims to compensate the reproducible part of the error.

ILC is often implemented in conjunction with a feedback controller. In general the sampled data system architecture of the feedback control system is exploited. Hence, the equidistant quantized measurement data at the sample frequency of the feedback control system is used in typical ILC implementations, [15].

The central idea in this paper is to employ exact data at the time-stamps, which is not corrupted by quantization, to obtain an increase in performance. This is facilitated by offline computations in ILC.

C.2. Eliminating quantization in ILC: exploiting time-stamps

Time-stamped measurement data does not suffer from quantization effects. Hence, exploiting this data in ILC can lead to a breakthrough in performance. There is no need for real-time computability in ILC, which allows the use of measurement data obtained at a higher sampling rate as the feedback controller [9].

Time-stamped ILC leads to several control issues. The non-equidistant measurement data leads to a linear time varying (LTV) system [15]. Moreover, the sequence of time-stamps will vary in the trial domain, which causes variation in the available number of discrete-data points. These challenges are all appropriately addressed in the present paper.

This leads to the formulation of the time-stamped ILC problem: use the available exact information $\bar{e}$ and corresponding time-stamps $\bar{t}$, in an appropriate criteria to design an ILC controller that generates u^l.

III. Time-stamped ILC

In this section the time-stamped ILC framework is developed. The following notation is adopted. The length of a trial is N^l samples corresponding to the control input. A signal x during the j-th trial is denoted by x_j. The sequence of time-stamps during the j-th trial is denoted by $\tau_j = (\bar{t}_1, \bar{t}_2, ..., \bar{t}_{m_j})$, here $\bar{t}_i$ is the sample corresponding to the i-th line transition, and m_j the number of time-stamps in the j-th trial. The sequence of time-stamps τ_j varies in the iteration domain. Due to the finite-length of a trial, there exists a finite number of possible sequences τ, the set containing all possible sequences τ is denoted by $\mathcal{T}$.

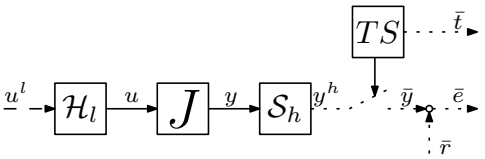

Fig. 4: Multirate time-stamped ILC setup

A. Assumptions

First, several assumptions are imposed.

Assumption III.1 *The sampling frequencies f_h and f_l satisfy $f_h = Mf_l, M \in \mathbb{N}$.*

Assumption III.2 *At each time-stamp $\bar{t}_i \in t$, the error $|y(\bar{t}_i) - \bar{y}(\bar{t}_i)| = 0$.*

Assumption III.3 *The sequence of time-stamps $\bar{t}_j$ in the j-th trial is assumed to be independent of the control input u_j.*

As the length of a trial is given to be $N_l \in \mathbb{N}$ samples of the feedback control system, this corresponds to $N_h = MN_l$ samples of the encoder. Assumption III.1 ensures that $N_h \in \mathbb{N}$. Assumption III.2 defines ideal time stamping, in analogy to the ideal sampler [10]. Assumption III.3 allows for performance guarantees through a worst-case analysis.

B. Time-stamped ILC setup

Consider the setup depicted in Fig. 4, where

$$y = Ju, \tag{5}$$

where J denotes a causal and stable continuous-time system, which can be either an open-loop or closed-loop system. The input of the system is denoted by $u = \mathcal{H}_l u^l$ with sampling frequency f_l corresponding to the sampling frequency of the feedback controller, see (4). The position output y is sampled using $\mathcal{S}_h$ to obtain y^h. Here, $\mathcal{S}_h$, is an ideal sampler with a sampling frequency of f^h corresponding to the frequency of the high-rate clock in the encoder, see Section II-A. Each trial the time-stamper TS determines the sequence of time-stamps $\tau := (\bar{t}_1, \bar{t}_2, ..., \bar{t}_m)$, see for example Fig. 2, and selects only these elements from y^h to obtain the position at the time-stamps denoted by $\bar{y}$, such that

$$\text{TS} : \bar{y}(i) = y^h(\bar{t}_i), i \in \{1, 2, ..., m\}. \tag{6}$$

The error at the time-stamps $\bar{e}$ is determined by subtracting the disturbance $\bar{r}$. This disturbance is obtained from a continuous-time iteration-invariant disturbance r such that $\bar{r}(i) = r(h_h \bar{t}_i)$ where $h_h = \frac{1}{f_h}$.

Next, the time-stamped ILC problem is defined.

Definition III.4 (Time-stamped ILC) Given the time-stamped ILC setup determine $u^l_{j+1} = F_{\tau_j}(u^l_j, \bar{e}_j)$ such that

either the sequence of error signals $\{e_j^h\}_{j\in\mathbb{Z}_{\geq 0}}$ or the sequence of input signals $\{u_j^l\}_{j\in\mathbb{Z}_{\geq 0}}$ converges monotonically.

C. Monotonic convergence of time-stamped ILC

Time-stamped ILC system has both time-varying behaviour in the time-domain, due to the non-equidistant measurement data during a trial, and in the iteration-domain since the sequence of time-stamps varies.

C.1. Iteration-invariant time-stamped ILC

First, the time-stamped ILC setup with solely time-varying behaviour in the time-domain is considered, i.e., $\tau_j = \bar{\tau} \in \mathcal{T}$. This reduces the time-stamped ILC problem to the following.

Definition III.5 (Iteration-invariant time-stamped ILC) Given the ILC setup with

$$e_j^h = \mathcal{S}_h r - \mathcal{S}_h J \mathcal{H}_l u_j^l. \tag{7}$$

and fixed sequence of time-stamps $\tau_j = \bar{\tau} \in \mathcal{T}, j \in \mathbb{Z}_{\geq 0}$, determine $u_{j+1}^l = F_{\bar{\tau}}(u_j^l, e_j^h(\bar{\tau}))$ such that either the sequence of error signals $\{e_j^h\}_{j\in\mathbb{Z}_{\geq 0}}$ or the sequence of input signals $\{u_j^l\}_{j\in\mathbb{Z}_{\geq 0}}$ converges monotonically, see Definition I.1.

Several methods are available to design an ILC controller for this type of ILC setups, including [16], [15].

C.2. Iteration-varying time-stamped ILC

Next the time-stamped ILC problem with time-varying behaviour in both the iteration domain and time-domain is considered, i.e. Definition III.4.

It is assumed that iteration-invariant time-stamped ILC problem III.5 is solved for each $\bar{\tau} \in \mathcal{T}$ by applying the ILC controller $F_{\bar{\tau}}$. Corresponding to each iteration-invariant time-stamped ILC setup, the point to which the error e^h and u^l converge are denoted by $e^h_{\bar{\tau},\infty}$ and $u^l_{\bar{\tau},\infty}$, respectively.

Note that, when applying the ILC controller F_{τ_j} during the j-th trial the norm $\|e_j^h - e^h_{\tau_j,\infty}\|_p$ (or $\|u_j^l - u^l_{\tau_j,\infty}\|_p$) is reduced by the ILC controller. Since, sequence of time-stamps τ_j varies in the iteration-domain, the point $e_{\tau_j,\infty}$ (or $u_{\tau_j,\infty}$) to which the system aims to converge varies each iteration. If $e^h_{\bar{\tau},\infty} \neq e^h_{\tilde{\tau},\infty}$ for some $\bar{\tau}, \tilde{\tau} \in \mathcal{T}$, monotonic convergence towards a fixed point cannot be guaranteed. Hence, the notion of monotonic convergence towards a p-norm ball is introduced:

Definition III.6 (Monotonic convergence towards a closed p-norm ball) A sequence $\{Y_i\}_i \in \mathbb{Z}_{\geq 0}$, $Y_i \in X$ is said to convergence monotonically, in a given p-norm, to the p-norm ball $\mathcal{B}_p(c,d), c \in X, d \in \mathbb{R}_{\geq 0}$ if there exists a $\kappa \in [0,1)$ such that

$$\|Y_{j+1} - c\|_p \leq \kappa \|Y_j - c\|_p \qquad \text{if } Y_j \notin \mathcal{B}_p(c,d), \tag{8}$$

$$Y_{j+1} \in \mathcal{B}_p(c,d) \qquad \text{if } Y_j \in \mathcal{B}_p(c,d), \tag{9}$$

are satisfied for all $j \in \mathbb{Z}_{\geq 0}$.

Remark III.7 Monotonic convergence towards the closed p-norm ball $\mathcal{B}_p(c,d)$ implies monotonic convergence towards each closed p-norm ball $\mathcal{B}_p(\bar{c},\bar{d})$ such that $\mathcal{B}_p(c,d) \subset \mathcal{B}_p(\bar{c},\bar{d})$. This leads to the aim of finding the smallest p-norm ball for which monotonic convergence is satisfied in order to conclude on the behaviour of the system as $j \to \infty$.

This leads to contribution C2, given by the following.

Theorem III.8 *Consider for each $\bar{\tau} \in \mathcal{T}$ the iteration-invariant time-stamped ILC setup with ILC controller $F_{\bar{\tau}}$, see Definition III.5. Moreover, consider the iteration varying time-stamped ILC setup with the ILC controller given by F_{τ_j}, see Definition III.4. Then the following two statements are equivalent for any given p-norm:*

(i) The sequence of errors $\{e_j^h\}_{j\in\mathbb{Z}_{\geq 0}}$ of the iteration-invariant time-stamped ILC systems with fixed $\tau_j = \bar{\tau} \in \mathcal{T}$ converge monotonically to a fixed point, see Definition I.1,

(ii) The sequence of errors $\{e_j^h\}_{j\in\mathbb{Z}_{\geq 0}}$ of the iteration-varying time-stamped ILC system is monotonically convergent towards a closed p-norm ball, see Definition III.6.

Furthermore, equivalence of (i) and (ii) holds when considering the sequence $\{u_j\}_{j\in\mathbb{Z}_{\geq 0}}$ instead of the sequence $\{e_j\}_{j\in\mathbb{Z}_{\geq 0}}$.

As mentioned in Remark (III.7) finding the smallest set $\mathcal{B}_p(c,d)$ is of interest when assessing the performance of the ILC controller when $j \to \infty$. The performance in terms of the size of the closed p-norm ball for a given ILC controller can be analysed using the following Theorem.

Theorem III.9 *For each $\bar{\tau} \in \mathcal{T}$ consider the iteration-invariant time-stamped ILC systems with corresponding ILC controller $F_{\bar{\tau}}$, see Definition III.5. Denote the convergence rate of each iteration-invariant time-stamped ILC system by $\kappa_{\bar{\tau}}$ and the point to which this system converges by $e_{\bar{\tau}\infty} \in \ell_p$. Moreover, consider the iteration-varying time-stamped ILC system with ILC controller $F_{\bar{\tau}_j}$, see Definition III.4. The smallest closed p-norm ball to which the iteration-varying time-stamped ILC system converges is given by $\mathcal{B}_p(c,d)$, where $c \in \ell_p$ and $d \in \mathbb{R}_{\geq 0}$ are the solution of the following optimization problem:*

$$\min_{c\in\ell_p, d\in\mathbb{R}_{\geq 0}} d \text{ s.t.} \tag{10a}$$

$$\frac{1+\kappa_{\bar{\tau}}}{1-\kappa_{\bar{\tau}}}\|e_{\bar{\tau}\infty} - c\|_p \geq d, \bar{\tau} \in \mathcal{T} \tag{10b}$$

When considering monotonic convergence of the sequence $\{u_j\}_{j\in\mathbb{Z}_{\geq 0}}$ instead of the sequence $\{e_j\}_{j\in\mathbb{Z}_{\geq 0}}$ a parallel result can be obtained.

For common used p-norms, such as the 1-norm, 2-norm, ∞-norm this optimization problem can be written as a semidefinite program (SDP) [17].

Notice that Theorem III.8 reduces the problem of designing a time-stamped ILC controller, to the design of a ILC controller $F_{\bar{\tau}}$ for each iteration-invariant time-stamped ILC problem, see Definition III.5. Hence, existing LTV ILC design techniques can be exploited. Moreover, the performance for $j \to \infty$ can be analysed by using the performance measures $e_{\bar{\tau}\infty}$ and $\kappa_{\bar{\tau}}$, of the individual iteration-invariant time-stamped ILC systems, as described by Theorem III.9. In the next section, these results are exploited to synthesize a time-stamped ILC controller.

IV. Time-Stamped ILC Design

In this section, a design approach for time-stamped ILC is introduced that is reminiscent to a typical norm-optimal ILC

approach. This allows for a direct comparison and shows the potential of time-stamped ILC.

A. Finite-time description

First the finite-time system description is introduced. Consider the system $\underline{J}^{h,h} = \mathcal{S}_h J \mathcal{H}_h$ with Markov parameters $m^h_{t_i}$, operating over a finite time interval $t_i \in [0, N_h] \subseteq t$, where the state of the system is reset to zero after each trial. The input-output behaviour is represented by its convolution matrix $\underline{J}^{h,h} \in \mathbb{R}^{N_h \times N_h}$ which maps the input vector $\underline{u}^h \in \mathbb{R}^{N_h}$ to output the output vector $\underline{y}^h \in \mathbb{R}^{N_h}$ [18], [19]:

$$\underline{y}^h = \underline{J}^{h,h}\underline{u}^h, \quad \underline{J}^{h,h} = \begin{bmatrix} m^h_0 & & 0 \\ \vdots & \ddots & \\ m^l_{N^l-1} & \dots & m^l_0 \end{bmatrix} \tag{11}$$

Moreover, define the finite-time description of the down sampler $\mathcal{H}_{h,l}$ as $\underline{\mathcal{H}}_h = I_M \otimes \mathbb{I}_M$ where $\mathbb{I}_M := \begin{bmatrix} 1 \dots 1 \end{bmatrix}^\top \in \mathbb{R}^M$ and $\otimes$ denotes the Kronecker product [20]. From this the finite-time description of $\underline{J}^{h,l} = \mathcal{S}_h J \mathcal{H}_l$ is given by

$$\underline{J}^{h,l} = \underline{J}^{h,h}\underline{\mathcal{H}}_{h,l}. \tag{12}$$

Moreover, a finite-time system description is defined for the time-stamp operator TS. Define for each $\bar{\tau} \in \mathcal{T}$, a mapping $\underline{T}_{\bar{\tau}} \in \mathbb{R}^{m \times N_h}$, that maps the error vector $\underline{e}^h \in \mathbb{R}^{N_h}$ to the error vector at the time-stamps $\bar{\underline{e}}(\bar{\tau}) \in \mathbb{R}^m$

$$\bar{\underline{e}}(\bar{\tau}) = \underline{T}_{\bar{\tau}}\underline{e}^h, \quad T_{\bar{\tau}} = \begin{bmatrix} \epsilon^\top_{t_1} & \epsilon^\top_{t_2} & \dots & \epsilon^\top_{t_m} \end{bmatrix}^\top \tag{13}$$

where $\epsilon_k, k \in \mathbb{Z}_{\geq 0}$ is a row vector of length N_l with 1 in the k-th position and 0 in every other position.

Using these definitions the finite-time description of the multi-rate time-stamped ILC setup is given by

$$\begin{aligned} \underline{u}_{j+1} &= F_{\tau_j}(\underline{u}_j, \underline{T}_{\tau_j}\underline{e}^h_j) \\ \underline{e}^h_j &= \underline{r}^h - \underline{J}^{h,l}\underline{u}_j \\ \tau_j &\in \mathcal{T} \end{aligned} \tag{14}$$

B. Design of time stamped ILC controller to achieve monotonic convergence in the 2-norm

Norm-optimal ILC, e.g., 2-norms is among the most popular ILC methodologies [1]. One common used method is designing a $\underline{Q}$ and $\underline{L}$ such that

$$\underline{u}_{j+1} = \underline{Q}\underline{u}_j + \underline{L}\underline{e}_j \tag{15}$$

such that the sequence of input signals $\{u_j\}_{j \in \mathbb{Z}_{\geq 0}}$ converges monotonically towards a fixed point in the 2-norm [1].

Inspired by ILC controller (15), the following ILC controller is proposed for (14),

$$\underline{u}_{j+1} = \underline{Q}\underline{u}_j + \underline{L}\,\underline{T}^\top_{\tau_j}\bar{\underline{e}}_j \tag{16}$$

where the matrices $\underline{Q}$ and $\underline{L}$ should be chosen such that the sequence of input signals $\{u_j\}_{j \in \mathbb{Z}_{\geq 0}}$ converges monotonically to a closed 2-norm ball. Due to the use of the 2-norm an LMI based convergence analysis and controller design method can be exploited [21]. Exploiting Theorem (III.8) this leads to the LMI conditions given in the following Theorem.

Theorem IV.1 *Consider the finite-time time-stamped ILC system* (14) *and the ILC controller of the form* (16)*, then the sequence of input signals $\{u_j\}_{j \in \mathbb{Z}_{\geq 0}}$ converges monotonically, in the 2-norm, to the set $\mathcal{B}_2(c, d)$ if $\underline{Q}$ and $\underline{L}$ satisfy the following linear matrix inequality (LMI)*

$$\begin{bmatrix} I & \underline{Q} - \underline{L}\underline{T}^\top_{\bar{\tau}}\underline{T}_{\bar{\tau}}\underline{J}^{h,l} \\ \underline{Q}^\top - (\underline{L}\underline{T}^\top_{\bar{\tau}}\underline{T}_{\bar{\tau}}\underline{J}^{h,l})^\top & I \end{bmatrix} \succ 0 \tag{17}$$

for each $\bar{\tau} \in \mathcal{T}$. With $c \in \mathbb{R}^{N_l}$ and $d \in \mathbb{R}_{\geq 0}$ the solution to the following optimization problem

$$\begin{aligned} &\min_{c \in \mathbb{R}^{N_l}, d \in \mathbb{R}_{\geq 0}} \quad d \quad \textit{s.t.} \\ &\begin{bmatrix} I & \underline{u}_{\bar{\tau}\infty} - c \\ \underline{u}^\top_{\bar{\tau}\infty} - c^\top & d^2\frac{(1-\kappa_{\bar{\tau}})^2}{(1+\kappa_{\bar{\tau}})^2} \end{bmatrix} \succ 0 \textit{ for all } \bar{\tau} \in \mathcal{T} \end{aligned} \tag{18}$$

where $\kappa_{\bar{\tau}}$ and $\underline{u}_{\bar{\tau}\infty}$ denote the convergence rate and fixed point to which the sequence of input signals $\{\underline{u}_j\}_{j \in \mathbb{Z}_{\geq 0}}$ converges, of the iteration-invariant time-stamped ILC system with $\tau_j = \bar{\tau} \in \mathcal{T}, j \in \mathbb{N}$, see definition III.5.

Remark IV.2 The matrix inequality in (18) can be converted to an LMI by fixing the value of d. Hence, the optimal c and d can be obtained by solving a semidefinite program (SDP) along a line-search algorithm for d. Note that when increasing the length of a trial the size of the set $\mathcal{T}$ increases exponentially. Hence, increasing the trial length leads to a significant increase in computation time of (18). Approaches that mitigate this are beyond the scope of the present paper and will be published elsewhere.

The results presented in Theorem IV.1 allow for computationally tractable algorithms to synthesize a time-stamped ILC controller and analyse the corresponding performance.

V. Numerical Example

In this section, the design approach introduced in Section IV are applied to a mass-spring-damper system, with the following transfer function $J(s) = \frac{1}{ms^2+cs+k}$ where the mass m, damping coefficient c, and spring constant k are all scaled to unity. The sampling frequencies of the control input and encoder are, $f_l = 1$ and $f_h = 3$, respectively. The aim of this example is to find an input u^l such that the position of the mass follows the reference r, given by the black line in Fig. 5c. The position measurement is quantized by an incremental encoder with an accuracy of 0.05. The intention of this example is to show the potential of time-stamped ILC. Hence, the trial length is chosen to be three samples long to facilitate the presentation and also to obtain a small computation time.

A traditional quantized ILC controller (15) and a time-stamped ILC controller (16) are designed using the finite-description as discussed in Section IV. The traditional quantized ILC controller exploits the quantized data available at the sampling frequency of the control input. The traditional quantized ILC controller is given by (15) with $Q = I_3$ and $L = (J^{l,l})^\dagger$. The time-stamped ILC controller developed in this paper, exploits the exact data that is available at the time stamps, and is determined using Theorem IV.1.

A. Simulation Results

he convergence results of the control input u^l_j and e^h_j are depicted in Fig. 5a and Fig. 5b, respectively. Clearly, the time-stamped ILC controller achieves higher performance, as

the error norm $\|e_j^h\|$ of time-stamped ILC reaches a lower value compared to traditional quantized ILC. Moreover, the control input u^l does not reach the theoretical u_∞^l, where the control input of time-stamped ILC clearly reaches inside the closed p-norm ball $\mathcal{B}_2(c,d)$ indicated by the dashed black line in Fig. 5a. It can be observed that $\{e_h^l\}_{j\in\mathbb{Z}_{\geq 0}}$ does not converge monotonically as only monotonic convergence of the sequence $\{u_j^l\}_{j\in\mathbb{Z}_{\geq 0}}$ is guaranteed. In Fig. 5c the position of the mass-spring-damper system in the 30-th trial is given for both ILC controllers. The discrete data points used by both ILC controllers are indicated. It can be observed that the quantization effect causes a measurement error. Although there is an error, this error is not visible due to the quantization of the measurement data available at the original quantized ILC controller. This error would be visible when exploiting the measurement data at the time-stamps.

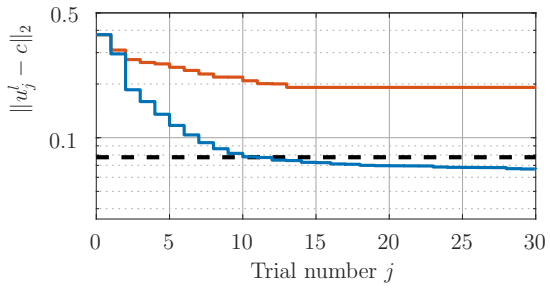

(a) Norm $\|u_j^l - u_\infty\|_2$ when applying traditional quantized ILC (—) and norm $\|u_j^l - c\|_2$ when applying time-stamped ILC of Section III (—). The edge of the sub-optimal 2-norm ball $\mathcal{B}_p(c,d)$ is indicated by the dashed black line (- -)

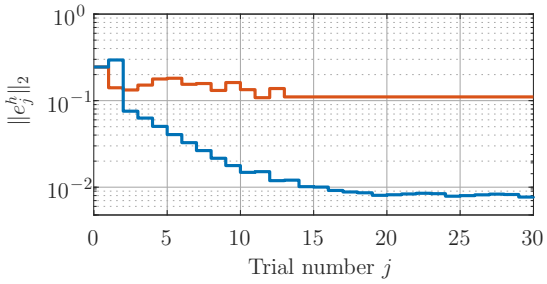

(b) Error norm $\|e_j^h\|_2$ when applying traditional quantized ILC (—) and the time-stamped ILC of Section III (—).

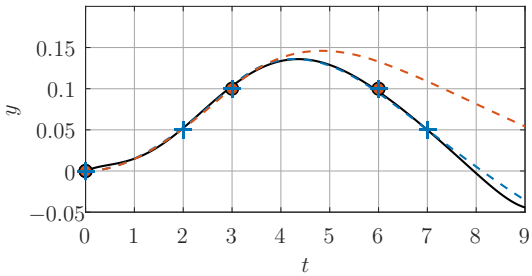

(c) Reference r (—) and the position of mass-spring-damper system during the 30-th trial when applying traditional quantized ILC (- -) and time-stamped ILC of Section III(- -). The equidistant data points used by quantized ILC are indicated by red marked dots(●); the data points used in time-stamped ILC are indicated by blue crosses (+).

Fig. 5: Simulation results.

VI. Conclusions

The key aspect brought forward in this paper is the role of quantization in ILC. A time-stamped ILC framework is introduced that eliminates quantization errors by exploiting exact non-equidistant measurement data. A theoretical framework for convergence and performance analysis of time-stamped ILC setups is provided. Moreover, a design procedure for a time-stamped ILC controller is outlined which ensures monotonic convergence in the 2-norm. Potentially large improvement can be achieved, since traditional ILC may amplify effects of quantization, as is also shown in the present paper.

References

[1] D. A. Bristow, M. Tharayil, and A. G. Alleyne, "A survey of iterative learning control," *IEEE Control Systems Magazine*, vol. 26, pp. 96–114, June 2006.

[2] K. L. Moore, *Iterative learning control for deterministic systems*. Springer Science & Business Media, 2012.

[3] G. F. Franklin, J. D. Powell, A. Emami-Naeini, and J. D. Powell, *Feedback control of dynamic systems*, vol. 3. Addison-Wesley Reading, MA, 1994.

[4] N. Strijbosch, L. Blanken, and T. Oomen, "Frequency domain design of iterative learning control and repetitive control for complex motion systems," in *IEEJ International Workshop on Sensing, Actuation, Motion Control, and Optimization (SAMCON), Tokyo, Japan*, 2018.

[5] J. C. Aguero, G. C. Goodwin, and J. I. Yuz, "System identification using quantized data," in *Decision and Control, 2007 46th IEEE Conference on*, pp. 4263–4268, IEEE, 2007.

[6] S. Gunnarsson and M. Norrlöf, "On the design of ILC algorithms using optimization," *Automatica*, vol. 37, no. 12, pp. 2011 – 2016, 2001.

[7] T. Oomen and C. R. Rojas, "Sparse iterative learning control with application to a wafer stage: Achieving performance, resource efficiency, and task flexibility," *Mechatronics*, vol. 47, pp. 134 – 147, 2017.

[8] R. H. Brown and S. C. Schneider, "Velocity observations from discrete position encoders," in *Signal Acquisition and Processing*, vol. 858, pp. 1111–1119, International Society for Optics and Photonics, 1987.

[9] T. Oomen, J. van de Wijdeven, and O. Bosgra, "Suppressing intersample behavior in iterative learning control," *Automatica*, vol. 45, no. 4, pp. 981 – 988, 2009.

[10] T. Chen and B. A. Francis, *Optimal sampled-data control systems*. Springer-Verlag London, 1995.

[11] A. J. Fleming and K. K. Leang, *Design, modeling and control of nanopositioning systems*. Springer, 2014.

[12] R. K. Miller, A. N. Michel, and J. A. Farrell, "Quantizer effects on steady-state error specifications of digital feedback control systems," *IEEE Trans. on Autom. Control*, vol. 34, pp. 651–654, June 1989.

[13] D. F. Delchamps, "Stabilizing a linear system with quantized state feedback," *IEEE Transactions on Automatic Control*, vol. 35, pp. 916–924, Aug 1990.

[14] R. Merry, M. van de Molengraft, and M. Steinbuch, "Optimal higher-order encoder time-stamping," *Mechatronics*, vol. 23, no. 5, pp. 481 – 490, 2013.

[15] J. van Zundert and T. Oomen, "On inversion-based approaches for feedforward and ILC," *Mechatronics*, vol. 50, pp. 282 – 291, 2018.

[16] H. Sun and A. G. Alleyne, "A computationally efficient norm optimal iterative learning control approach for LTV systems," *Automatica*, vol. 50, no. 1, pp. 141 – 148, 2014.

[17] S. Boyd and L. Vandenberghe, *Convex optimization*. Cambridge university press, 2004.

[18] J. A. Frueh and M. Q. Phan, "Linear quadratic optimal learning control (LQL)," *Int. Journal of Control*, vol. 73, no. 10, pp. 832–839, 2000.

[19] M. Phan and R. Longman, "A mathematical theory of learning control for linear discrete multivariable systems," in *Astrodynamics Conference*, p. 4313, 1988.

[20] K. Zhou, J. C. Doyle, K. Glover, *et al.*, *Robust and optimal control*, vol. 40. Prentice hall New Jersey, 1996.

[21] K. Galkowski, J. Lam, E. Rogers, S. Xu, B. Sulikowski, W. Paszke, and D. Owens, "LMI based stability analysis and robust controller design for discrete linear repetitive processes," *Int. Journal of Robust and Nonlinear Control*, vol. 13, no. 13, pp. 1195–1211, 2003.